

Geophysical Research Letters®

RESEARCH LETTER

10.1029/2021GL093796

Special Section:

The COVID-19 pandemic:
linking health, society and
environment

Key Points:

- Aerosols reduced by COVID-19 lockdown perturbed atmospheric heat budget over the Indo-Gangetic Plain
- Cloud optical thickness and cloud-particle effective radius increased during COVID-19 lockdown period
- Air temperature in the lower troposphere decreased during COVID-19 lockdown period

Supporting Information:

Supporting Information may be found in the online version of this article.

Correspondence to:

P. Khatri,
pradeep.khatri.a3@tohoku.ac.jp

Citation:

Khatri, P., Hayasaka, T., Holben, B., Tripathi, S. N., Misra, P., Patra, P. K., et al. (2021). Aerosol loading and radiation budget perturbations in densely populated and highly polluted Indo-Gangetic Plain by COVID-19: Influences on cloud properties and air temperature. *Geophysical Research Letters*, 48, e2021GL093796. <https://doi.org/10.1029/2021GL093796>

Received 9 APR 2021

Accepted 2 OCT 2021

Aerosol Loading and Radiation Budget Perturbations in Densely Populated and Highly Polluted Indo-Gangetic Plain by COVID-19: Influences on Cloud Properties and Air Temperature

P. Khatri^{1,2} , T. Hayasaka¹ , B. Holben³, S. N. Tripathi⁴ , P. Misra² , P. K. Patra^{1,2,5} , S. Hayashida², and U. C. Dumka⁶ 

¹Graduate School of Science, Center for Atmospheric and Oceanic Studies, Tohoku University, Sendai, Japan, ²Research Institute for Humanity and Nature, Kyoto, Japan, ³National Aeronautics and Space Administration, Goddard Space Flight Center, Greenbelt, MD, USA, ⁴Department of Civil Engineering, Indian Institute of Technology Kanpur, Kanpur, India, ⁵Research Institute for Global Change, JAMSTEC, Yokohama, Japan, ⁶Aryabhata Research Institute of Observational Sciences (ARIES), Nainital, India

Abstract Aerosols emitted in densely populated and industrialized Indo-Gangetic Plain, one of the most polluted regions in the world, modulate regional climate, monsoon, and Himalayan glacier retreat. Thus, this region is important for understanding aerosol perturbations and their resulting impacts on atmospheric changes during COVID-19 lockdown period, a natural experimental condition created by the pandemic. By analyzing 5 years (2016–2020) data of aerosols and performing a radiative transfer calculation, we found that columnar and near-surface aerosol loadings decreased, leading to reductions in radiative cooling at the surface and top of the atmosphere and atmospheric warming during lockdown period. Further, satellite data analyses showed increases in cloud optical thickness and cloud-particle effective radius and decrease in lower tropospheric air temperature during lockdown period. These results indicate critical influences of COVID-19 lockdown on regional climate and water cycle over Indo-Gangetic Plain, emphasizing need for further studies from modeling perspectives.

Plain Language Summary The COVID-19 control measures constrained human activities, reducing anthropogenic emissions around the world, including Indo-Gangetic Plain (IGP), one of the global aerosol hotspots. Aerosols emitted in the IGP can affect regional climate, water cycle, Himalayan glacier retreat, etc. Thus, understanding the impacts of COVID-19 lockdown in aerosol field and other associated components of the atmosphere over IGP is important for better understanding the roles of aerosols on climate and water cycle of South Asia and its vicinity. This study suggests reductions of both near-surface and columnar aerosol loadings by lockdown measures further reduced radiative cooling at the surface and top of the atmosphere and atmospheric warming. The effects were also noted in the cloud field by increasing cloud optical thickness and cloud-particle effective radius and in the meteorological field by reducing air temperature in the lower troposphere. These manifold impacts over this important source region indicate broad influences of COVID-19 on the regional climate and water cycle, underscoring further investigations.

1. Introduction

The current coronavirus infection (COVID-19), first identified in December 2019, spread rapidly throughout the world in a very short time forcing the World Health Organization (WHO) to declare global pandemic in March 2020. Preventive measures have been (are being) taken to suppress the virus spread by controlling social and commercial activities. Despite health crisis, economic loss, and social inconveniences, the COVID-19 preventive measures are leading to reductions in air pollution, non-COVID-19 deaths, and air pollution related diseases (Chen et al., 2020; Dhaka et al., 2020).

In the past, short-term/city-scale pollution reduction campaigns, such as “Olympic Blue” for 2008 Beijing Summer Olympic Games (Wang et al., 2010) and “APEC Blue” for 2014 Asia-Pacific Economic Cooperation (APEC) Economic Leaders’ meeting (Huang et al., 2015), showed improvements in air quality after

controlling human activities. The COVID-19 lockdown drastically constrained human activities on a scale larger than those campaigns, providing a good opportunity to revisit a less polluted atmosphere to understand the level of human engagement in degrading the environment and climate. This resulted in an exponential increase of COVID-19 related studies after the outbreak, mostly focusing on the degree of air quality improvement (e.g., Dumka et al., 2021; Manchanda et al., 2021; Mishra et al., 2021; Misra et al., 2021; Wetchayont et al., 2021). Aerosols affect the climate by scattering and absorbing solar radiation (direct effect) (e.g., Coakley et al., 1983), changing the atmospheric stability and burning clouds (semi-direct effect) (e.g., Hansen et al., 1997), and modifying the cloud microphysical and optical properties (indirect effect) (e.g., Albrecht, 1989; Twomey, 1977). Despite a large volume of studies, the impacts of COVID-19 lockdown on such multifaceted effects of aerosols have not been studied in details. A numerical model simulation by Yang et al. (2020) showed surface warming over the continental regions of the Northern Hemisphere due to reduction of aerosols during the COVID-19 pandemic. However, a similar modeling study of Jones et al. (2021) suggests no detectable impact of COVID-19 pandemic on near-surface temperature or rainfall during 2020–2024 in their initial analysis. Jones et al. (2021) emphasized the necessity of regional analyses on a finer scale, and closer attention to extremes (especially linked to changes in atmospheric composition and air quality) to test the impact of COVID-19-related emission reductions on near-term climate. This underscores the necessity of studying the consequences of COVID-19 lockdown on different aerosol effects by using observation-based data.

The long-term and high-quality observation data, such as aerosol optical properties (AOPs) observed by Aerosol Robotic Network (AERONET) (Holben et al., 1998), offer a great opportunity for such studies. This has motivated us to use AERONET and other auxiliary data to investigate the impact of COVID-19 lockdown on aerosol loading and its consequences to other changes in the atmosphere. We chose Indo-Gangetic Plain (IGP) for our study. IGP is one of the most densely populated and highly polluted regions in the world (Mhawish et al., 2020) with a very complex mixture of natural and anthropogenic aerosols (e.g., Gautam et al., 2011; Srivastava et al., 2011). These aerosols play very important roles on Himalayan glacier retreat (Li et al., 2016; Sarangi et al., 2020), Indian summer monsoon modulation (Patra et al., 2005; Sanap et al., 2015), etc., indirectly affecting the water cycle, agriculture, economy, and lives of people residing in Asia.

2. Data

AOPs (aerosol optical depth (AOD), single scattering albedo (SSA), and asymmetry parameter (ASY)) and surface reflectance at 440-nm, 675-nm, 870-nm, and 1,020-nm wavelengths along with columnar precipitable water content (PWC) of cloudless sky conditions were obtained from AERONET. We used data of two typical sites of IGP: Indian Institute of Technology (IIT), Kanpur (26.513°N, 80.232°E), an urban site (hereafter referred as IIT Kanpur) and Gandhi College (25.871°N, 84.128°E), Ballia, a rural site. As Level 2.0 data for full study period (2016–2020) are currently unavailable, Level 1.5 (version 3) data (Giles et al., 2019; Sinyuk et al., 2020) were processed by following the quality control procedures of Holben et al. (2006).

We further used Modern-Era Retrospective Analysis Research and Applications, Version 2 (MERRA-2) aerosol data assimilated from Goddard Earth Observing System-5 (GEOS-5) atmospheric general circulation model (Molod et al., 2015) coupled with Goddard Chemistry Aerosol Radiation and Transport (GOCART) model (Chin et al., 2002) and aerosol observations from space. The GOCART model simulates the global distributions of dust, sea-salt, black carbon, organic carbon, and sulfate taking into account emissions, chemical reactions for sulfate precursors, advection, boundary layer turbulent mixing, moist convection, and depositions, as described in detail by Chin et al. (2002). The MERRA-2 aerosol data are available at a horizontal resolution of 0.5°(latitude) × 0.625°(longitude) at 1-hourly time interval. The near-surface particulate matter with aerodynamic diameter (d) < 2.5 μm ($PM_{2.5}$) was calculated as (Navinya et al., 2020)

$$PM_{2.5} = 1.375 \times [SO_4] + 1.8 \times [OC] + [BC] + [DU_{2.5}] + [SS_{2.5}] \quad (1)$$

where $[SO_4]$, $[OC]$, $[BC]$, $[DU_{2.5}]$, and $[SS_{2.5}]$ are mass concentrations for sulfate, organic carbon, black carbon, dust with $d < 2.5$ μm, and sea-salt with $d < 2.5$ μm, respectively. The conversion factors of 1.375 for SO_4 (Chow et al., 2015) and 1.8 for OC (Hand et al., 2013) are for reconstructing mass concentrations of $(NH_4)_2SO_4$ (inorganic ion) and organic matter, respectively. The poorly constrained emissions and physical process parameterizations in the model and uncertainties in the observation data are major error sources

in MERRA-2 $PM_{2.5}$ (Buchard et al., 2016; Randles et al., 2017). However, several studies (e.g., Buchard et al., 2016, 2017; He et al., 2019; Randles et al., 2017; Song et al., 2018) demonstrated a good capability of MERRA-2 to capture the spatial and temporal variations of $PM_{2.5}$.

We further used Level 3 (collection 6.1) cloud properties (cloud optical depth (COD), cloud-particle effective radius (CER), and cloud fraction; Platnick et al., 2017) and AODs at 550 nm (Gupta et al., 2020) observed by Moderate Resolution Spectroradiometer (MODIS) aboard Terra and Aqua satellites and Level 3 (version 7.0) vertical profiles of air temperature observed by Atmospheric Infrared Sounder (AIRS) aboard Aqua satellite (Kalmus et al., 2015). They are daily products with spatial resolution of $1^\circ \times 1^\circ$.

3. Methodology

From the daily mean values of spectral AOP and surface reflectance along with PWC, downwelling and upwelling global radiative fluxes (spectral range: 0.3–3.0 μm) at the surface and top of the atmosphere (TOA) were calculated for 15-min interval of 5 a.m.–7 p.m. (local time) of each day for both aerosol-free and aerosol-laden atmospheres by using the Santa Barbara DISORT Atmospheric Radiative Transfer (SBDART) model (Ricchiazzi et al., 1998). Assuming solar flux as 0 W m^{-2} for time falling outside of 5 a.m.–7 p.m., the net (downwelling-upwelling) fluxes of 15-min interval were integrated to calculate 24-h mean values of aerosol radiative forcing (ARF) at the surface (ARF_Surface) and TOA (ARF_TOA). ARF is defined as the difference between net fluxes of aerosol-free and aerosol-laden atmospheres. The 24-h mean atmospheric forcing (ATM) was calculated as the difference between ARF_TOA and ARF_Surface. Note that the sunrise and sunset are after 5 a.m. and before 7:15 p.m. throughout the year at both sites (<https://www.timeand-date.com/astronomy/india>). If the sunrise is after 5 a.m. and/or the sunset is before 7 p.m., the calculated fluxes in between 5 a.m. and sunrise and/or 7 p.m. and sunset should be 0 W m^{-2} . Similarly, the maximum deviation up to 15 min, if the sunset is after 7 p.m., merely affects the calculated values because of low solar altitude just before the sunset. The mean of daily mean values of AOD, $PM_{2.5}$, and those quantified radiative effects (QREs) of first 4 years (2016–2019) were compared with those for 2020 to access the change of each in 2020. As the focus of this study is to understand the impacts of COVID-19 lockdown, intensive analyses were done for lockdown period of 25 March to 30 June 2020 (day number of the year: 85–182) (Misra et al., 2021) and the coincident periods of previous years (2016–2019).

4. Results and Discussion

4.1. Perturbations in Aerosol Loading

Figures 1a–1d show time series of AOD at 440 nm (upper) and $PM_{2.5}$ (lower) for 2016–2019 (blue) and 2020 (red) for IIT Kanpur (left) and Gandhi College (right). The peaks and valleys in AOD and $PM_{2.5}$ time series are consistent to each other at both sites. This suggests local sources as important contributors of columnar aerosol loading at both sites. Both $PM_{2.5}$ and AOD were high in the winter season (December–February) because of meteorological conditions, including shallow boundary layer and air stagnation (Ojha et al., 2020). Aerosol loadings of both column atmosphere and near-surface dropped clearly during lockdown period. This suggests that lockdown measures decreased aerosol loading over IGP, though high relative humidity increased AOD over central India during lockdown period (Pandey & Vinoj, 2021). AOD and $PM_{2.5}$ values for lockdown period of 2020 were less than those corresponding to 2016–2019 by 25% each at IIT Kanpur and by 33% and 29%, respectively, at Gandhi College (Table 1). Despite such decrease, Table 1 suggests still considerably high values of AOD and $PM_{2.5}$ over study areas. For reference, Dubovik et al. (2002) showed AOD (440 nm) of 0.24–0.43 range for AERONET sites representing the urban-industrial and mixed atmospheres. The WHO recommended 24-h mean $PM_{2.5}$ for clean air is $25 \mu\text{g}/\text{m}^3$. Of note, MERRA-2 $PM_{2.5}$ can be lower than ground-truth $PM_{2.5}$ (e.g., Navinya et al., 2020), suggesting that actual $PM_{2.5}$ values over the study areas could be higher than those summarized in Table 1. Considering that industrial and transportation sectors were under control during lockdown period, the mean values of AOD for 2020 for IIT Kanpur and Gandhi College, shown in Table 1, might represent a typical scenario over IGP with influences from only household sector and natural sources. Such high AODs during lockdown period could result from two important reasons: dense population of IGP and influence of natural dust aerosols. The dense population can result regional high AOD (Ramachandran & Cherian, 2008; Wang et al., 2017). Recent studies (e.g., Bonardi

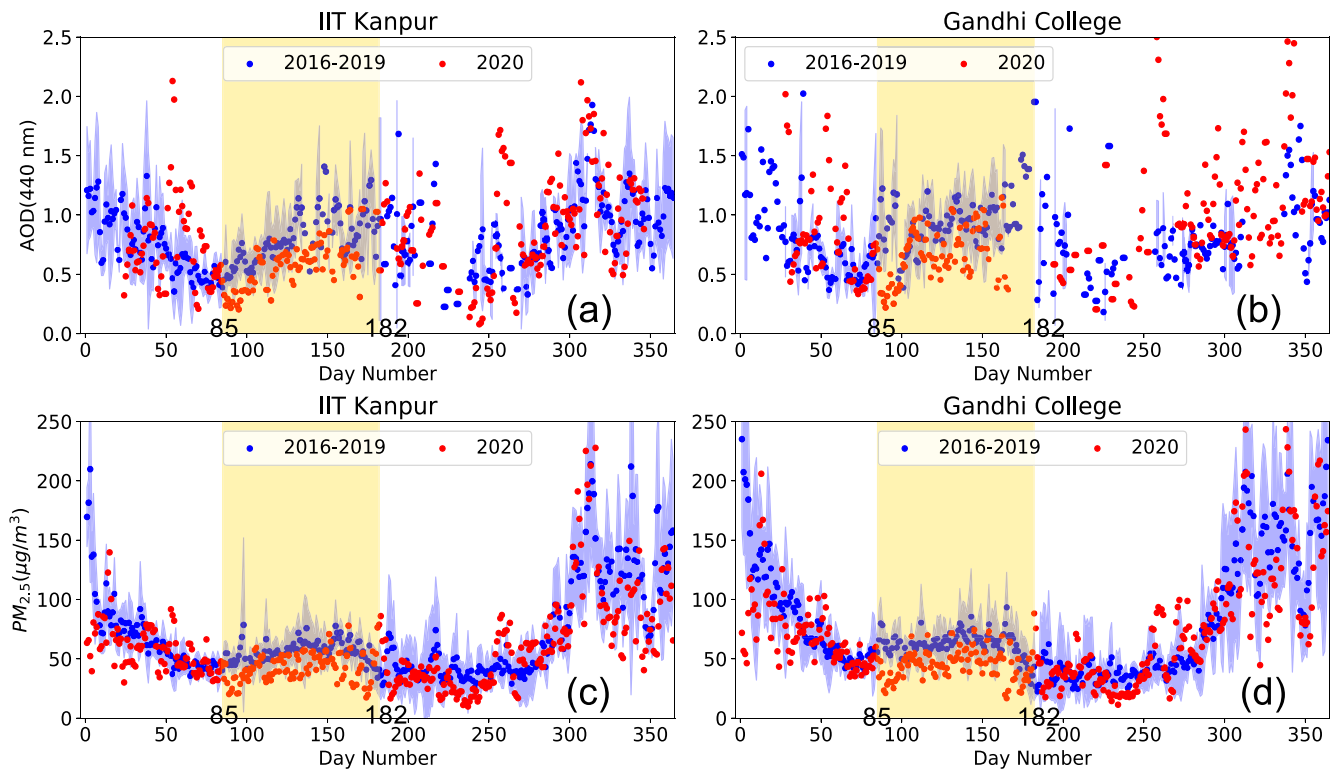


Figure 1. Time series of aerosol optical depth (AOD) at 440 nm (upper) and MERRA-2 $PM_{2.5}$ (lower) for IIT Kanpur (left) and Gandhi College (right) for 2016–2019 (blue circles and shadow show the mean and standard deviation values, respectively) and 2020 (red circles). Data gaps are seen, as the measurements are available only for clear sky conditions. The yellow-shaded area in between day numbers 85 and 182 represents lockdown period.

et al., 2021; Khatri & Hayasaka, 2021) showed a weak influence of lockdown measures on household air pollutant reduction, suggesting that such high AOD could be possible over densely populated IGP even without active emissions from commercial and transportation sectors. As there was decrease in AOD over upwind regions during lockdown period (Pandey & Vinoj, 2021), such high AODs were less likely due to the effects of human activities of upwind regions. Further, IGP is a region prone to natural dust aerosols during premonsoon season to increase AOD (e.g., Gautam et al., 2011). Nonetheless, Table 1 suggests reductions of near-surface and total column aerosol loadings by less than one-third of the mean values for 2016–2019. These reductions were still insufficient to meet WHO recommendation, suggesting household sector as important source of aerosol emission over IGP. Further, aerosols increased gradually after lockdown period, suggesting the immediate revive of commercial sectors after lockdown.

Table 1
Mean of Daily Mean Values of Aerosol Optical Properties and Quantified Radiative Effects During Lockdown Period of 2020 and Same Periods of Previous Years

Year/ parameter	AOD (440 nm)	MERRA-2 $PM_{2.5}$ ($\mu\text{g}/\text{m}^3$)	SSA (440 nm)	AAOD (440 nm)	ARF_Surface (W m^{-2})	ARF_TOA (W m^{-2})	ATM (W m^{-2})
Site: IIT Kanpur (26.513°N, 80.232°E)							
2016–2019	0.76 ± 0.29	55.82 ± 17.6	0.89 ± 0.03	0.08 ± 0.03	-36.42 ± 11.04	-8.52 ± 4.68	27.9 ± 10.86
2020	0.57 ± 0.21	41.98 ± 12.17	0.90 ± 0.03	0.06 ± 0.02	-29.88 ± 7.36	-6.18 ± 3.0	23.7 ± 7.39
Site: Gandhi College (25.871°N, 84.128°E)							
2016–2019	0.92 ± 0.27	62.7 ± 19.36	0.89 ± 0.05	0.08 ± 0.03	-45.62 ± 14.16	-7.98 ± 7.83	37.64 ± 18.5
2020	0.62 ± 0.22	44.5 ± 12.41	0.89 ± 0.02	0.06 ± 0.02	-34.67 ± 9.61	-5.84 ± 2.56	28.83 ± 9.39

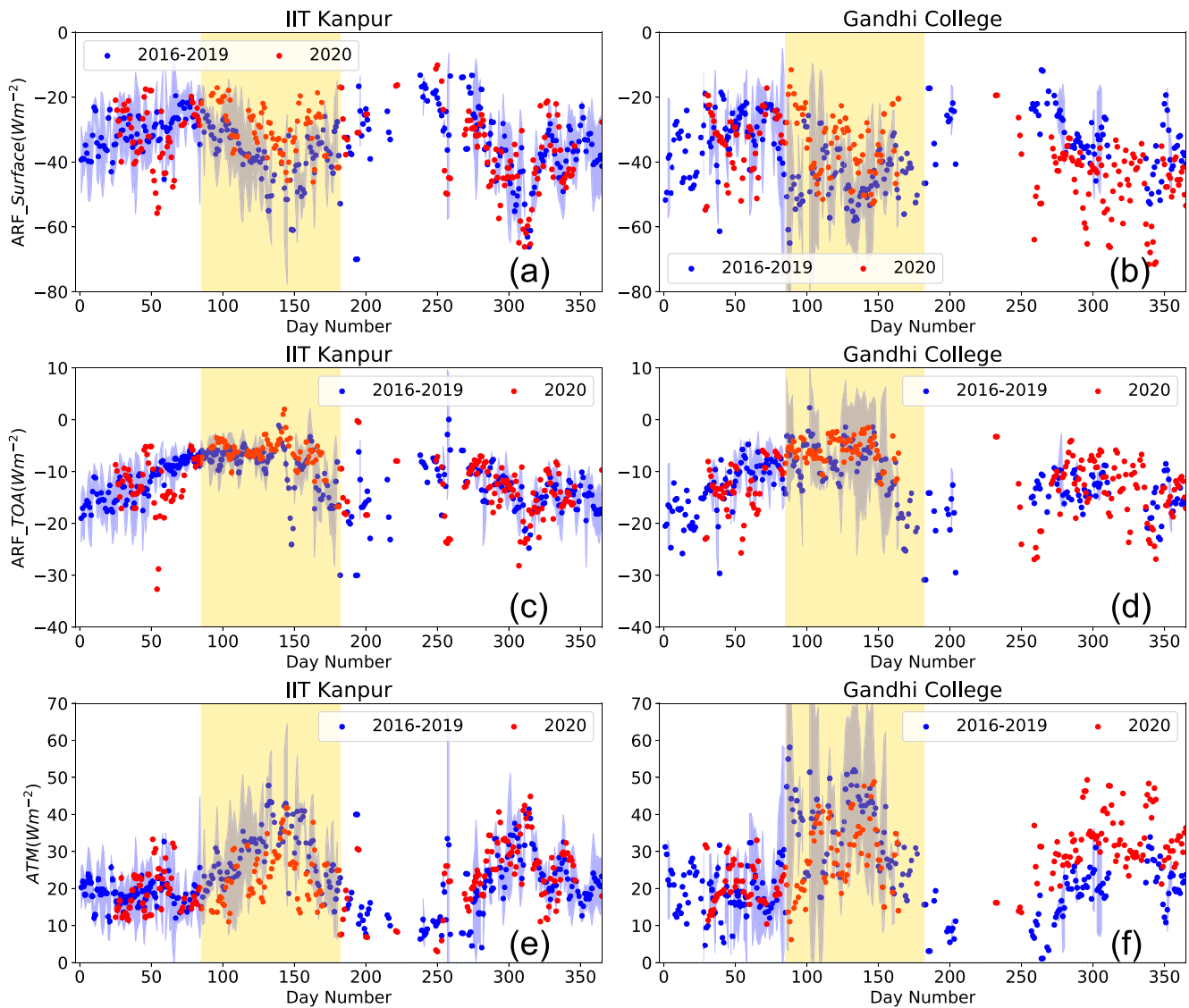


Figure 2. Same as Figure 1, but for time series of aerosol radiative forcing (ARF) at the surface (upper), ARF at top of the atmosphere (TOA; middle), and atmospheric forcing (lower) for spectral range of 0.3–3.0 μm .

Unlike AOD, no remarkable influence of lockdown measures can be seen on SSA, a measure of aerosol light-absorption capacity, in Table 1. This result indicates internally mixed aerosols over IGP. Previously, Srivastava and Ramachandran (2013) suggested core-shell mixing as the probable mixing state of aerosols over IGP. The absorption optical thickness (AAOD), i.e., $\text{AOD} \times (1 - \text{SSA})$, decreased by around 25% at each site (Table 1) during lockdown period. Brief descriptions of SSA and AAOD time series are given in Text S1 in Supporting Information S1.

4.2. Perturbations in Shortwave Radiation Budget

Same as Figure 1, Figures 2a–2f show time series of ARF_Surface, ARF_TOA, and ATM, respectively, for IIT Kanpur (left) and Gandhi College (right). The correlation coefficient (r) values for QRE and AOP correlations are given in Table 2 for both sites. Among different AOPs (AOD, SSA, and ASY at 440 nm; the values of Angstrom Exponent, a parameter describing the wavelength dependence, for AOD (Ext. Ang.) and SSA (SSA Ang.)), AOD and SSA were important in determining QRE, as revealed from Table 2. The role of ASY (the average cosine of the scattering angles, defining the degree of forward scattering) was weaker than

Table 2
Correlation Coefficients for the Relations of Aerosol Optical Properties and Quantified Radiative Effects

QRE/AOP	AOD (440 nm)	SSA (440 nm)	ASY (440 nm)	Ext. Ang. Exp.	SSA Ang. Exp.
Site: IIT Kanpur (26.513°N, 80.232°E)					
ARF_Surface	-0.86	0.15	-0.1	0.07	-0.01 ^a
ARF_TOA	-0.82	-0.62	0.01 ^a	-0.3	0.31
ATM	0.53	-0.53	0.12	-0.25	0.18
Site: Gandhi College (25.871°N, 84.128°E)					
ARF_Surface	-0.77	0.42	-0.19	0.16	0.08
ARF_TOA	-0.58	-0.77	-0.08	-0.3	0.09
ATM	0.44	-0.72	0.14	-0.28	-0.03 ^a

^aStatistically insignificant at the 95% confidence level.

the roles of AOD and SSA. Similarly, the role of Ext. Ang. was relatively stronger than that for SSA Ang. The correlations of these two important AOPs (AOD and SSA) with QREs are shown in Figures S2 and S3 in Supporting Information S1. The increase of AOD tended to decrease ARF_Surface and ARF_TOA, but tended to increase ATM (Figure S2 in Supporting Information S1); whereas, the increase of SSA tended to increase ARF_Surface, but tended to decrease ARF_TOA and ATM (Figure S3 in Supporting Information S1). Thus, the peaks and valleys in time series of ARF_Surface (Figures 2a and 2b) and ATM (Figures 2e and 2f) were closely coincident with those in time series of AOD (Figures 1a and 1b). However, the peaks and valleys of ARF_TOA time series (Figures 1c and 1d) coincided closely with neither AOD (Figures 1a and 1b) nor SSA time series (Figures S1a and S1b in Supporting Information S1) because of competing effects of AOD and SSA on ARF_TOA. Table 1 suggests that ARF_Surface (ARF_TOA) for lockdown period of 2020 was higher than that corresponding to 2016–2019 by around 18% (27%) and 24% (27%) for IIT Kanpur and Gandhi College, respectively. But, ATM for the lockdown period of 2020 was lower than that corresponding to 2016–2019 by 15% and 9% for IIT Kanpur and Gandhi College, respectively. Such perturbations in aerosol radiative effects during lockdown period primarily resulted from AOD perturbations because SSAs were merely influenced by lockdown measures, as discussed above and shown in Table 1.

4.3. Influences on Cloud Properties and Air Temperature

The COVID-19 lockdown led changes in aerosol field could affect not only radiation field, but also cloud properties and meteorology. We accessed remotely sensed cloud and air temperature data to understand the signatures of COVID-19 lockdown on cloud and meteorological fields. The mean values of water cloud properties (COD and CER) and air temperature profile within $1^\circ \times 1^\circ$ grid including our study areas are shown in Figure 3 for lockdown period of 2020 and same periods of previous years. The mean values of COD (CER) in previous years were less than the value in 2020 by 18–40% (10–23%) and 19–46% (9–18%) over IIT Kanpur and Gandhi College, respectively (Figures 3a and 3b). The temporal variations of COD and CER are described in Text S2 in Supporting Information S1. Though there are different pathways for aerosols to influence clouds (see Text S3 in Supporting Information S1), those values suggest different cloud fields in 2020 than in previous years, which can be discussed in light of decreased AOD in 2020. The size decrement and number concentration increment of water cloud-droplets due to aerosol increment can lead more water mass aloft in the atmosphere to form ice particles by releasing latent heat once the freezing level is reached. This can invigorate cloud vertical development and expansion. This phenomenon, known as Aerosol Invigoration Effect (AIE; Khatri et al., 2020; Rosenfeld et al., 2014), in 2020 could have been weakened by suppressing the decrement of water cloud-droplet size and conversion of water cloud into ice cloud because of decreased aerosols. Further, light-absorbing aerosols can reduce cloud cover and droplet size by warming and stabilizing the lower atmosphere (Hansen et al., 1997) and embedding within clouds (Jacobson, 2012). Such cloud burning efficiency (aerosol semi-direct effect) in 2020 could have been suppressed because of reduced AOD (or AAOD), resulting higher COD and CER in 2020 than in previous years. Text S3 in Supporting Information S1 discusses AIE and aerosol semi-direct effect over our study areas to support these results. Next, Figures 3c and 3d show that air temperature profiles from 2016 to 2019 were very close to each other, although the profile for 2020 was different from them. The vertical profiles for the difference between temperature of 2020 and the mean value for 2016–2019, shown by dashed lines, clarify the decrease of air temperature in the lower troposphere (>400 hPa) in 2020 over both study areas. Though the roles of factors other than aerosols may not be negligible, absorbing aerosols are capable to modulate air temperature profile, as suggested by Myhre et al. (2013). We speculate that decreased ATM as well as increased COD and CER due to AOD (and AAOD) reduction played important roles to reduce air temperatures in the lower troposphere in 2020. A detailed modeling study in future may shed further light on the link between aerosol reduction and air temperature change. Nonetheless, Figure 3 provides observation-based evidences to suggest that COVID-19 lockdown could have also affected cloud and meteorological fields over the IGP.

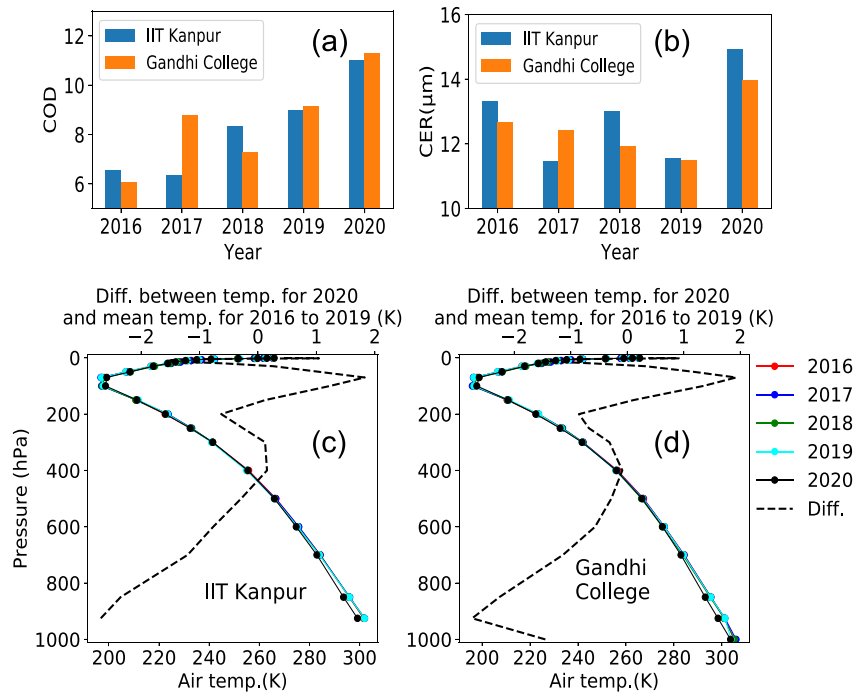


Figure 3. Water cloud (a) Cloud optical depth (COD) and (b) Cloud-particle effective radius (CER) for IIT Kanpur and Gandhi College and vertical profiles of air temperature (solid lines) for (c) IIT Kanpur and (d) Gandhi College for lockdown period of 2020 and same periods of previous years. The dashed line shows the difference between temperature profile of 2020 and the mean profile for 2016–2019.

Accounting such multidimensional impacts of COVID-19 lockdown over this important source region, it is reasonable to suggest that the climate system of South Asia could have been affected by COVID-19 led perturbations in aerosol loading.

5. Conclusion

The COVID-19 lockdown measures restricted human activities, resulting to improve air quality. The lockdown measures have further influenced the environment and climate system in different ways far beyond air quality improvement only, which are yet to be understood in detail. Taking advantage of ground-truth AERONET observations over two typical sites (IIT Kanpur and Gandhi College) of densely populated and highly polluted IGP, one of the most important aerosol sources in the world, the COVID-19 lockdown brought influences in aerosol loading and radiation budget and thereby in cloud properties and air temperature were investigated using AERONET, reanalysis, and satellite data and radiative transfer calculation. The COVID-19 lockdown measures reduced aerosol loadings of column atmosphere and near-surface by about one-fourth to one-third of the mean values for 2016–2019 to reduce the surface (TOA) cooling by 18–24% (30–30%) and atmospheric heating by 9–15% at those two distinctly distant (around 450 km) regions. Further, cloud properties (COD and CER) were found to have increased with decreased air temperature in the lower troposphere (>400 hPa) during lockdown period of 2020 at both regions. Such signatures of COVID-19 lockdown over this important source region indicate its manifold impacts in the environment and climate system of South Asia and vicinity, underscoring need for more detailed investigations in future from both observation and modeling perspectives.

Data Availability Statement

AERONET and MERRA-2 data were downloaded from <https://aeronet.gsfc.nasa.gov> and <https://goldsmr4.gesdisc.eosdis.nasa.gov/data/MERRA2/>, respectively. MODIS and AIRS data were downloaded from <https://giovanni.gsfc.nasa.gov/giovanni/>.

Acknowledgments

This study was supported by the Research Institute for Humanity and Nature (RIHN: a constituent member of NIHU) Project No. 14200133 (Aakash), “Virtual Laboratory for Diagnosing the Earth’s Climate System” program of MEXT, Japan, and Grant-in-Aid for Scientific Research (C) 17K05650 from JSPS, Japan. SNT acknowledges financial supports from Department of Biotechnology (DBT) (Grant No. BT/IN/UK/APHH/41/KB/2016-17) and Central Pollution Control Board (CPCB) (Grant No. AQM/Source apportionment Project/2017), Government of India. Thanks to the three reviewers for their constructive comments and suggestions.

References

- Albrecht, B. A. (1989). Aerosols, cloud microphysics, and fractional cloudiness. *Science*, *245*, 1227–1230. <https://doi.org/10.1126/science.245.4923.1227>
- Bonardi, J. P., Gallea, Q., Kalanoski, D., Lalive, R., Madhok, R., Noack, F., et al. (2021). Saving the world from your couch: The heterogeneous medium-run benefits of COVID-19 lockdowns on air pollution. *Environmental Research Letters*, *16*, 074010. <https://doi.org/10.1088/1748-9326/abee4d>
- Buchard, V., da Silva, A. M., Randles, C. A., Colarco, P., Ferrare, R., Hair, J., et al. (2016). Evaluation of the surface PM_{2.5} in Version 1 of the NASA MERRA aerosol reanalysis over the United States. *Atmospheric Environment*, *125*, 100–111. <https://doi.org/10.1016/j.atmosenv.2015.11.004>
- Buchard, V., Randles, C. A., da Silva, A. M., Darmenov, A., Colarco, P. R., Govindaraju, R., et al. (2017). The MERRA-2 aerosol reanalysis, 1980 onward. Part II: Evaluation and case studies. *Journal of Climate*, *30*(17), 6851–6872. <https://doi.org/10.1175/jcli-d-16-0613.1>
- Chen, K., Wang, M., Huang, C., Kinney, P. L., & Anastas, P. T. (2020). Air pollution reduction and mortality benefit during the COVID-19 outbreak in China. *The Lancet Planetary Health*, *4*(6), e210–e212. [https://doi.org/10.1016/s2542-5196\(20\)30107-8](https://doi.org/10.1016/s2542-5196(20)30107-8)
- Chin, M., Ginoux, P., Kinne, S., Torres, O., Holben, B. N., Duncan, B. N., et al. (2002). Tropospheric aerosol optical thickness from the GOCART model and comparisons with satellite and sun photometer measurements. *Journal of the Atmospheric Sciences*, *59*, 461–483. [https://doi.org/10.1175/1520-0469\(2002\)059<0461:TAOTFT>2.0.CO;2](https://doi.org/10.1175/1520-0469(2002)059<0461:TAOTFT>2.0.CO;2)
- Chow, J. C., Lowenthal, D. H., Chen, L. W., Wang, X., & Watson, J. G. (2015). Mass reconstruction methods for PM_{2.5}: A review. *Air Quality, Atmosphere, and Health*, *8*(3), 243–263. <https://doi.org/10.1007/s11869-015-0338-3>
- Coakley, J. A., Jr., Cess, R. D., & Yurevich, F. B. (1983). The effect of tropospheric aerosols on the Earth’s radiation budget: A parameterization for climate models. *Journal of the Atmospheric Sciences*, *40*(1), 116–138. [http://doi.org/10.1175/1520-0469\(1983\)040<0116:teotao>2.0.co;2](http://doi.org/10.1175/1520-0469(1983)040<0116:teotao>2.0.co;2)
- Dhaka, S. K., Chetna, Kumar, V., Panwar, V., Dimri, A. P., Singh, N., et al. (2020). PM_{2.5} diminution and haze events over Delhi during the COVID-19 lockdown period: An interplay between the baseline pollution and meteorology. *Scientific Reports*, *10*(1), 13442. <https://doi.org/10.1038/s41598-020-70179-8>
- Dubovik, O., Holben, B., Eck, T. F., Smirnov, A., Kaufman, Y. J., King, M. D., et al. (2002). Variability of absorption and optical properties of key aerosol types observed in worldwide locations. *Journal of the Atmospheric Sciences*, *59*, 590–608. [https://doi.org/10.1175/1520-0469\(2002\)059<0590:VOAAOP>2.0.CO;2](https://doi.org/10.1175/1520-0469(2002)059<0590:VOAAOP>2.0.CO;2)
- Dumka, U. C., Kaskaoutis, D. G., Verma, S., Ningombam, S. S., Kumar, S., & Ghosh, S. (2021). Silver linings in the dark clouds of COVID-19: Improvement of air quality over India and Delhi metropolitan area from measurements and WRF-CHIMERE model simulations. *Atmospheric Pollution Research*, *12*(2), 225–242. <https://doi.org/10.1016/j.apr.2020.11.005>
- Gautam, R., Hsu, N. C., Tsay, S. C., Lau, K. M., Holben, B., Bell, S., et al. (2011). Accumulation of aerosols over the Indo-Gangetic Plains and southern slopes of the Himalayas: Distribution, properties and radiative effects during the 2009 pre-monsoon season. *Atmospheric Chemistry and Physics*, *11*(24), 12841–12863. <https://doi.org/10.5194/acp-11-12841-2011>
- Giles, D. M., Sinyuk, A., Sorokin, M. G., Schafer, J. S., Smirnov, A., Slutsker, I., et al. (2019). Advancements in the Aerosol Robotic Network (AERONET) Version 3 database—Automated near-real-time quality control algorithm with improved cloud screening for Sun photometer aerosol optical depth (AOD) measurements. *Atmospheric Measurement Techniques*, *12*(1), 169–209. <https://doi.org/10.5194/amt-12-169-2019>
- Gupta, P., Remer, L. A., Patadia, F., Levy, R. C., & Christopher, S. A. (2020). High-resolution gridded level 3 aerosol optical depth data from MODIS. *Remote Sensing*, *12*(17), 2847. <https://doi.org/10.3390/rs12172847>
- Hand, J. L., Schichtel, B. A., Malm, W. C., & Frank, N. H. (2013). Spatial and temporal trends in PM_{2.5} organic and elemental carbon across the United States. *Advances in Meteorology*, *2013*, 367674. <https://doi.org/10.1155/2013/367674>
- Hansen, J., Sato, M., & Ruedy, R. (1997). Radiative forcing and climate response. *Journal of Geophysical Research*, *102*(D6), 6831–6864. <https://doi.org/10.1029/96JD03436>
- He, L., Lin, A., Chen, X., Zhou, H., Zhou, Z., & He, P. (2019). Assessment of MERRA-2 surface PM_{2.5} over the Yangtze River Basin: Ground-based verification, spatiotemporal distribution and meteorological dependence. *Remote Sensing*, *11*(4), 460. <https://doi.org/10.3390/rs11040460>
- Holben, B. N., Eck, T. F., Slutsker, I., Smirnov, A., Sinyuk, A., Schafer, J., et al. (2006). AERONET’s Version 2.0 quality assurance criteria. In *Proceeding of SPIE 6408 remote sensing of the atmosphere and clouds* (p 64080Q). <https://doi.org/10.1117/12.706524>
- Holben, B. N., Eck, T. F., Slutsker, I., Tanré, D., Buis, J. P., Setzer, A., et al. (1998). AERONET—A federated instrument network and data archive for aerosol characterization. *Remote Sensing of Environment*, *66*, 1–16. [https://doi.org/10.1016/s0034-4257\(98\)00031-5](https://doi.org/10.1016/s0034-4257(98)00031-5)
- Huang, K., Zhang, X., & Lin, Y. (2015). The “APEC Blue” phenomenon: Regional emission control effects observed from space. *Atmospheric Research*, *164–165*, 65–75. <https://doi.org/10.1016/j.atmosres.2015.04.018>
- Jacobson, M. Z. (2012). Investigating cloud absorption effects: Global absorption properties of black carbon, tar balls, and soil dust in clouds and aerosols. *Journal of Geophysical Research*, *117*, D06205. <https://doi.org/10.1029/2011JD017218>
- Jones, C. D., Hickman, J. E., Rumbold, S. T., Walton, J., Lamboll, R. D., Skeie, R. B., et al. (2021). The climate response to emissions reductions due to COVID19: Initial results from CovidMIP. *Geophysical Research Letters*, *48*, e2020GL091883. <https://doi.org/10.1029/2020GL091883>
- Kalmus, P., Wong, S., & Teixeira, J. (2015). The pacific subtropical cloud transition: A MAGIC assessment of AIRS and ECMWF thermodynamic structure. *IEEE Geoscience and Remote Sensing Letters*, *12*(7), 1586–1590. <https://doi.org/10.1109/LGRS.2015.2413771>
- Khatrri, P., & Hayasaka, T. (2021). Impacts of COVID-19 on air quality over China: Links with meteorological factors and energy consumption. *Aerosol and Air Quality Research*, *21*, 200668. <https://doi.org/10.4209/aaqr.200668>
- Khatrri, P., Ooashi, H., & Iwabuchi, H. (2020). Investigating aerosol effects on maritime deep convective clouds using satellite and reanalysis data. *Sola*, *16*, 228–232. <https://doi.org/10.2151/sola.2020-038>

- Li, C., Bosch, C., Kang, S., Andersson, A., Chen, P., Zhang, Q., et al. (2016). Sources of black carbon to the Himalayan-Tibetan Plateau glaciers. *Nature Communications*, 7, 12574. <https://doi.org/10.1038/ncomms12574>
- Manchanda, C., Kumar, M., Singh, V., Faisal, M., Hazarika, N., Shukla, A., et al. (2021). Variation in chemical composition and sources of PM_{2.5} during the COVID-19 lockdown in Delhi. *Environment International*, 153, 106541. <https://doi.org/10.1016/j.envint.2021.106541>
- Mhawish, A., Banerjee, T., Sorek-Hamer, M., Bilal, M., Lyapustin, A. I., Chatfield, R., & Broday, D. M. (2020). Estimation of high-resolution PM_{2.5} over the Indo-Gangetic Plain by fusion of satellite data, meteorology, and land use variables. *Environmental Science and Technology*, 54(13), 7891–7900. <https://doi.org/10.1021/acs.est.0c01769>
- Mishra, G., Ghosh, K., Dwivedi, A. K., Kumar, M., Kumar, S., Chintalapati, S., & Tripathi, S. N. (2021). An application of probability density function for the analysis of PM_{2.5} concentration during the COVID-19 lockdown period. *Science of the Total Environment*, 782, 146681. <https://doi.org/10.1016/j.scitotenv.2021.146681>
- Misra, P., Takigawa, M., Khatri, P., Dhaka, S. K., Dimri, A. P., Yamaji, K., et al. (2021). Nitrogen oxides concentration and emission change detection during COVID-19 restrictions in North India. *Scientific Reports*, 11(1), 9800. <https://doi.org/10.1038/s41598-021-87673-2>
- Molod, A., Takacs, L., Suarez, M., & Bacmeister, J. (2015). Development of the GEOS-5 atmospheric general circulation model: Evolution from MERRA to MERRA2. *Geoscientific Model Development*, 8(5), 1339–1356. <https://doi.org/10.5194/gmd-8-1339-2015>
- Myhre, G., Myhre, C. E. L., Samset, B. H., & Storelvmo, T. (2013). Aerosols and their relation to global climate and climate sensitivity. *Nature Education Knowledge*, 4(5), 7. <https://www.nature.com/scitable/knowledge/library/aerosols-and-their-relation-to-global-climate-102215345>
- Navinia, C. D., Vinoj, V., & Pandey, S. K. (2020). Evaluation of PM_{2.5} surface concentrations simulated by NASA's MERRA version 2 aerosol reanalysis over India and its relation to the air quality index. *Aerosol and Air Quality Research*, 20(6), 1329–1339. <https://doi.org/10.4209/aaqr.2019.12.0615>
- Ojha, N., Sharma, A., Kumar, M., Girach, I., Ansari, T. U., Sharma, S. K., et al. (2020). On the widespread enhancement in fine particulate matter across the Indo-Gangetic Plain towards winter. *Scientific Reports*, 10(1), 5862. <https://doi.org/10.1038/s41598-020-62710-8>
- Pandey, S. K., & Vinoj, V. (2021). Surprising changes in aerosol loading over India amid COVID-19 lockdown. *Aerosol and Air Quality Research*, 21(3), 200466. <https://doi.org/10.4209/aaqr.2020.07.0466>
- Patra, P. K., Behera, S. K., Herman, J. R., Maksyutov, S., Akimoto, H., & Yamagata, Y. (2005). The Indian summer monsoon rainfall: Interplay of coupled dynamics, radiation and cloud microphysics. *Atmospheric Chemistry and Physics*, 5, 2181–2188. <https://doi.org/10.5194/acp-5-2181-2005>
- Platnick, S., Meyer, K., King, M. D., Wind, G., Amarasinghe, N., Marchant, B., et al. (2017). The MODIS cloud optical and microphysical products: Collection 6 updates and examples from terra and aqua. *IEEE Transactions on Geoscience and Remote Sensing*, 55, 502–525. <https://doi.org/10.1109/TGRS.2016.2610522>
- Ramachandran, S., & Cherian, R. (2008). Regional and seasonal variations in aerosol optical characteristics and their frequency distributions over India during 2001–2005. *Journal of Geophysical Research*, 113, D08207. <https://doi.org/10.1029/2007JD008560>
- Randles, C. A., Da Silva, A. M., Buchard, V., Colarco, P. R., Darmenov, A., Govindaraju, R., et al. (2017). The MERRA-2 aerosol reanalysis, 1980-onward, Part I: System description and data assimilation evaluation. *Journal of Climate*, 30(17), 6823–6850. <https://doi.org/10.1175/JCLI-D-16-0609.1>
- Ricchiazzi, P., Yang, S., Gautier, C., & Sowle, D. (1998). SBDART: A research and teaching software tool for plane-parallel radiative transfer in the Earth's atmosphere. *Bulletin of the American Meteorological Society*, 79, 2101–2114. [https://doi.org/10.1175/1520-0477\(1998\)079<2101:SARATS>2.0.CO;2](https://doi.org/10.1175/1520-0477(1998)079<2101:SARATS>2.0.CO;2)
- Rosenfeld, D., Andreae, M. O., Asmi, A., Chin, M., Leeuw, G., Donovan, D. P., et al. (2014). Global observations of aerosol-cloud-precipitation-climate interactions. *Reviews of Geophysics*, 52, 750–808. <https://doi.org/10.1002/2013RG000441>
- Sanap, S. D., Pandithurai, G., & Manoj, M. G. (2015). On the response of Indian summer monsoon to aerosol forcing in CMIP5 model simulations. *Climate Dynamics*, 45(9–10), 2949–2961. <https://doi.org/10.1007/s00382-015-2516-2>
- Sarang, C., Qian, Y., Rittger, K., Leung, L. B., Chand, D., Bormann, K. J., & Painter, T. H. (2020). Dust dominates high-altitude snow darkening and melt over high-mountain Asia. *Nature Climate Change*, 10, 1045–1051. <https://doi.org/10.1038/s41558-020-00909-3>
- Sinyuk, A., Holben, B. N., Eck, T. F., Giles, D. M., Slutsker, I., Korkin, S., et al. (2020). The AERONET Version 3 aerosol retrieval algorithm, associated uncertainties and comparisons to Version 2. *Atmospheric Measurement Techniques*, 13(6), 3375–3411. <https://doi.org/10.5194/amt-13-3375-2020>
- Song, Z., Fu, D., Zhang, X., Wu, Y., Xia, X., He, J., et al. (2018). Diurnal and seasonal variability of PM_{2.5} and AOD in North China plain: Comparison of MERRA-2 products and ground measurements. *Atmospheric Environment*, 191, 70–78. <https://doi.org/10.1016/j.atmosenv.2018.08.012>
- Srivastava, A. K., Tiwari, S., Devara, P. C. S., Bisht, D. S., Srivastava, M. K., Tripathi, S. N., et al. (2011). Pre-monsoon aerosol characteristics over the Indo-Gangetic Basin: Implications to climatic impact. *Annales Geophysicae*, 29(5), 789–804. <https://doi.org/10.5194/angeo-29-789-2011>
- Srivastava, R., & Ramachandran, S. (2013). The mixing state of aerosols over the Indo-Gangetic Plain and its impact on radiative forcing. *Quarterly Journal of the Royal Meteorological Society*, 139(670), 137–151. <https://doi.org/10.1002/qj.1958>
- Twomey, S. (1977). The influence of pollution on the shortwave albedo of clouds. *Journal of the Atmospheric Sciences*, 34, 1149–1152. [https://doi.org/10.1175/1520-0469\(1977\)034<1149:tiopot>2.0.co;2](https://doi.org/10.1175/1520-0469(1977)034<1149:tiopot>2.0.co;2)
- Wang, J. X., Wu, S. H., Zhou, S. L., & Tang, J. (2017). Relationship between aerosol optical depth and population density in typical area of east China. *Applied Ecology and Environmental Research*, 15(3), 1041–1056. https://doi.org/10.15666/aeer/1503_10411056
- Wang, S., Zhao, M., Xing, J., Wu, Y., Zhou, Y., Lei, Y., et al. (2010). Quantifying the air pollutants emission reduction during the 2008 Olympic games in Beijing. *Environmental Science and Technology*, 44(7), 2490–2496. <https://doi.org/10.1021/es9028167>
- Wetchayont, P., Hayasaka, T., & Khatri, P. (2021). Air quality improvement during COVID-19 lockdown in Bangkok metropolitan, Thailand: Effect of the long-range transport of air pollutants. *Aerosol and Air Quality Research*, 21, 200662. <https://doi.org/10.4209/aaqr.200662>
- Yang, Y., Ren, L., Li, H., Wang, H., Wang, P., Chen, L., et al. (2020). Fast climate responses to aerosol emission reductions during the COVID-19 pandemic. *Geophysical Research Letters*, 47, e2020GL089788. <https://doi.org/10.1029/2020GL089788>